Nanotechnology Science and Technology

SMART NANOOBJECTS

SYNTHESIS AND CHARACTERIZATION

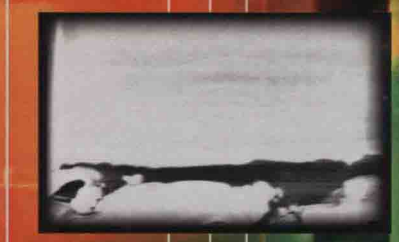

KIRILL LEVINE
EDITOR

NOVA

NANOTECHNOLOGY SCIENCE AND TECHNOLOGY

SMART NANOOBJECTS

SYNTHESIS AND CHARACTERIZATION

KIRILL LEVINE
EDITOR

nova publishers
New York

Library of Congress Cataloging-in-Publication Data

Smart nanoobjects : synthesis and characterization / editor: Kirill Levine.
pages cm
Includes bibliographical references and index.
ISBN 978-1-62618-431-2 (hardcover)
1. Smart materials. 2. Nanostructured materials. I. Levine, Kirill.
TA418.9.S62S5245 2013
620.1'15--dc23

2013009419

Published by Nova Science Publishers, Inc. † New York

NANOTECHNOLOGY SCIENCE AND TECHNOLOGY

SMART NANOOBJECTS

SYNTHESIS AND CHARACTERIZATION

NANOTECHNOLOGY SCIENCE AND TECHNOLOGY

Additional books in this series can be found on Nova's website under the Series tab.

Additional e-books in this series can be found on Nova's website under the e-book tab.

PREFACE

This book provides coverage of several actual topics in nanocomposite research: one-dimensional objects, nanotubes, coordinated metallic compounds, encapsulated nano and micro objects, and nanoobjects with sensor properties. It is oriented to both professionals and beginners in the field. This book provides awareness of the most recent developments in the scientific and practical areas of nanotechnology.

Chapter 1 – New series of Cu(II), Ni(II), Co(II), Cd(II), Mn(II), Zn(II), Fe(III) and Cr(III) of the 7,12-dioxo-3,4,9,10-tetraphenyl-1,2,5,6-tetraazacyclododeca-2,4,8,10-tetraene-8,11-dicarbonitrile, (H_2L), have been synthesized and characterized by elemental analyses, IR, UV-VIS, ^{1}H-NMR, mass and ESR spectra, magnetic susceptibility and molar conductivity measurements. The spectral data and magnetic measurements of the complexes indicate that, the ligand behaves either as neutral bidentate, monobasic bidentate, neutral tetradentate or bibasic tetradentate ligand. The geometries of the metal complexes are either square planar or octahedral. The antibacterial and antifungal activities of the compounds showed that, some of metal complexes exhibited a greater inhibitory effect than standard drugs (Tetracycline) for bacteria, (Amphotericin B) for fungi.

Chapter 2 – InMnAs layers, grown by pulse laser deposition at 320°C in the flux of hydrogen and arsine, represent a nanosystem with MnAs clusters. Ferromagnetic properties of the InMnAs layers up to room temperature were confirmed by the results of the anomalous Hall Effect and magnetization measurements. Resistivity dependence on temperature has semiconductor character. The dependences of the electrical and magnetic parameters of the layers on the Mn content were investigated.

Chapter 3 – Peptide nucleic acids (PNAs) are one of the promising antisense drugs for the gene therapy. PNAs are DNA mimics with the peptide-like backbone. PNAs form the most stable complementary duplexes with RNA among all known modified and non-modified oligonucleotides and have high exo- and endonuclease resistance. However, PNAs themselves cannot penetrate through cellular membranes. Here the authors propose to use nanocomposites based on titanium dioxide (TiO_2) nanoparticles for the delivery of PNAs into living cells. After delivery of antisense PNA drugs into the cells there is still a problem with PNA molecules release from nanocomposite vehicles in cytoplasm inside of cells. Here the authors designed special nanocomposites on the basis of TiO_2 nanoparticles (4-6 nm in diameter) containing the hybrid PNA\DNA duplexes. The attachment of PNA\DNA duplexes to nanoparticles preliminary covered with polylysine (PL) occurs due to the electrostatic interaction between negatively charged internucleotide phosphate groups of DNA and

positively charged amino groups of polylysine. It was demonstrated that the resulted TiO_2/PL/DNA/PNA nanocomposite can be delivered into the cells. Dissociation or release time of PNA from the DNA/PNA duplex attached to the nanocomposite was measured and easily could be regulated with the length of the overlap of complementary base pairs in the initially constructed DNA/PNA duplexes in nanocomposite TiO_2/PL/DNA/PNA. Thus, PNA/DNA complex with optimal overlap number or optimal half-release time of PNA from nanocomposite allows at least the half quantity of PNA still to remain in TiO_2/PL/DNA/PNA nanocomposite during the delivery and then able to be released from the nanocomposite after its delivery inside of the cells. These features of the constructed nanocomposites were demonstrated on the example of nanocomposites containing various overlap length of DNA/PNA duplexes (from 10 to 16 base pairs). It was found that the time of half-release of PNA from these TiO_2/PL/DNA/PNA nanocomposites changed from 10 to 70 min depended on overlap length of DNA/PNA duplexes in conditions close to physiological (35°C in PBS buffer, pH 7.5). The greater the overlap of the DNA/PNA duplex in nanocomposite TiO_2/PL/DNA/PNA, the longer the time of PNA release from this nanocomposite. Thus, the adjustable reversible method of PNA immobilization on TiO_2 nanoparticles was developed. Created PNA containing nanocomposites were capable to penetrate cell membranes without transfectants or other adverse procedures.

Chapter 4 – New closed form expression for the potential of single atom interacting by Lennard-Jones potential with the finite set of atoms situated on the straight line in the continuum approximation is presented. The developed expression has better accuracy then based on the same approach traditional one, because continuum integral is compared with the discreet sum of parabolic approximation. It is shown that the proposed potential gives better accuracy in the region of the edges of straight line, the region where classic continuum approach gives poor approximation. The proposed potential can be used for simulation of dynamics of such objects as carbon nanotubes, graphene flakes, Langmuir-Blodgett films etc.

Chapter 5 – Permanent magnets can produce large forces (mN) over long activation distances, which provide a significant advantage over the limited mN range force and short distance provided by electrostatic and thermal actuators. To achieve this advantage, the magnetic energy in the magnetized films should be maximized. One way to reach this objective is using magnets during electroplating. In this paper the authors analyze the effect of this alternative in films properties. Nevertheless the fracture occurence increased when films were deposited in the presence of magnetic field, roughness decreased and homogeneity increased.

Chapter 6 – This review will present a comprehensive view of the use of microcapsules in coatings. Beginning with the general self healing strategy, this paper will discuss the traditional repair methods used in polymers. It will then continue to summarize the recent advances in the field of smart materials pertaining to applications in coatings. The review summarizes the work of many research groups across the globe and presents the recent advances in the coatings industry with the incorporation of these smart microcapsules capable of performing various protective functions to increase the life time of the coatings chosen for the selected area of application.

Chapter 7 – Simulation results for Ga ion beam interaction with thin membranes of different materials (C, Si, Pt) are presented. Experiments with ion beam irradiation were carried out at different doses with suspended 50-100 nm thick multi-layer graphene (MLG) flakes. Cross-sectioning using focused ion beam milling revealed that material removal

occurs in areas 60-80 nm wide at the beam lateral dimension of 20 nm, being consistent with the results of TRIM simulations. Further studies with thinner MLG samples are in progress to achieve better ion beam processing resolution.

Chapter 8 – The azo ligands of sulfamethoxazole were prepared through coupling the sulfamethoxazole diazonium salt with each of resorcinol, ß-naphthol, salicylaldehyde and acetyl acetone to form H_2L^1, HL^2-HL^4 respectively. Different metal complexes of H_2L^1 with $CuCl_2$, $CoCl_2$, $NiCl_2$, $PtCl_2$, $RuCl_3$, $Cr(CO)_6$, and $Mo(CO)_6$ and metal complexes of HL^2 –HL^4 with $CuCl_2$ have been prepared and characterized using variety of analytical, spectral, magnetic and thermal techniques. The ligands were comprised of two compartments, so the study revealed that the prepared complexes except copper complex and the platinum complex were binuclear complexes. The study also showed that each compartment behaved either as a bidentate ligand either as a neutral or monobasic. The results of magnetic moment values and electronic spectra as well as other techniques indicate that all copper complexes and platinum complex exhibit square planar arrangement around the metal ion. The other complexes possess octahedral geometry. The thermal stability of some of the prepared complexes were also studied. The molecular weight of some metal complexes as well as their fragmentations have also been studied by mass spectra measurement.

Chapter 9 – Copper(II), nickel(II) and cobalt(II) complexes of of (3,3',4,4')-4,4'-(1,4-phenylenebis(azan-1-yl-1-ylidene))bis(3-(hydroxyimino)pentan-2-one) have been prepared by direct and template methods. The ligand and its complexes have been characterized by elemental analyses, spectroscopic technique as IR, UV. Vis., ESR, magnetic moment and conductivity measurements. The molar conductivity values of the complexes in DMF are commensurate with their non-electrolytic nature. The spectral data showed that the ligand act as neutral tetradentate or dibasic tetradentate ligand bonded to the metal ions throughall C=N and protonated or deprotonated C=N-O groups forming octahedral geometry around the metal ions. The ESR spectra of copper(II) complexes (9), (10) and (13) show $g_{\|}$-values (2.274, 2.282, 2.256) which commensurate with considerable covalent bond character with a d_{x2-y2} ground state.

Chapter 10 – Nickel(II), cobalt(II) and copper(II) complexes of dibasic ligands with two oxime groups have been synthesized and characterized by elemental analyses, molar conductance, magnetic moments, IR, UV-Vis. spectra, DTA, mass spectra, ^{1}H- and ^{13}C-NMR and ESR measurements. IR spectra showed that, the ligands behaved as dibasic ligands. Ni(II), d^8 complex was exposed to ^{60}Co-γ rays at 77 K using a 0.2217 M. rad. H^{-1} Vicrad source to give Ni(I), d^9, with a d_{x2-y2} ground state. Annealing the complex above 77 K led to the formation of a low spin Ni(III), d^7 system with d_z2 orbital. However, copper(II) complexes showed an axial type symmetry with a d_{x2-y2} ground state. The suggested structures of the ligands and their metal complexes are in accordance with analytical, spectral and magnetic moment data.

Chapter 11 – Novel metal complexes of 1-(5-(1-(((1H-benzo[d]imidazol-2-yl)methyl) imino)ethyl)-2,4-dihydroxyphenyl)ethanone, H_3L^1, 3-((E)-(1-(5-((E)-1-(((1H-benzo[d] imidazol-2-yl) methyl) imino) ethyl)-2,4-dihydroxyphenyl) ethylidene) amino)-2-thioxothia zolidin-4-one, H_3L^2 and 4,6-bis((E)-1-(((1H-benzo[d]imidazol-2-yl)methyl) imino)ethyl) benzene-1,3-diol, H_4L^3 with $Ag^{(I)}$, $Cu^{(II)}$, $Fe^{(III)}$, $Ru^{(III)}$, $Pt^{(II)}$, VO^{II}, $Ni^{(II)}$ have been prepared and characterized using physico-chemical and spectroscopic methods. The molar conductance data revealed that all complexes are non-electrolytes except complex 6, which behaved as a 1:1 electrolyte. IR data showed that H_3L^1 behaved as neutral tridentate ligand except in case

of complex 2, in which it behaved as neutral pentadentate ligand. Ligands H_3L^2 and H_4L^3 behaved as neutral hexadentate ligands. The spectral data and magnetic measurements of the complexes indicated that, the geometries are either square planar, square pyramidal or octahedral. The Copper complexes 3 and 15 showed a remarkable smaller value of IC50 than that of the Tamoxifen which would provide a new potential antitumor drug that deserves more attention.

Chapter 12 – Gas-sensitive nanocomposites based on silicon dioxide and tin dioxide were obtained via self-assembly by sol-gel method. Surface morphology of nanomaterials synthesized from sol solutions in medium of precursor based on tetraethoxysilane was characterized by atomic force microscopy. Formation approach of metal contacts adhered to hierarchical porous structure based on electroadhesion technology was proposed. The advantages of this technique were discussed, and the theoretical concepts of processes taking place during formation of adhesive contacts were considered. Electrical properties of nanomaterials based on porous silicon with the introduced metal oxide nanocomposites were studied by impedance spectroscopy. Gas-sensitive properties of synthesized samples were measured.

CONTENTS

In: Smart Nanoobjects
Editor: Kirill Levine

ISBN: 978-1-62618-431-2

Chapter 1

SYNTHESIS, SPECTROSCOPIC INVESTIGATION AND ANTIMICROBIAL STUDIES OF METAL COMPLEXES OF 7,12-DIOXO-3,4,9,10-TETRAPHENYL-1,2,5,6-TETRAAZACYCLODODECA-2,4,8,10-TETRAENE-8,11-DICARBONITRILE

Abdou S. El-Tabl*[*1], Ahemd M. A. El-Seidy[2], Mohamad M. E. Shakdofa[2] and Alaa El-Deen A. I. Hamdy[1]

[1]Department of Chemistry, Faculty of Science,
El-Menoufia University, Shebin El-Kom, Egypt
[2]Inorganic Chemistry Department,
National Research Center, Dokki, Cairo, Egypt

ABSTRACT

New series of Cu(II), Ni(II), Co(II), Cd(II), Mn(II), Zn(II), Fe(III) and Cr(III) of the 7,12-dioxo-3,4,9,10-tetraphenyl-1,2,5,6-tetraazacyclododeca-2,4,8,10-tetraene-8,11-dicarbonitrile, (H_2L), have been synthesized and characterized by elemental analyses, IR, UV-VIS, ^{1}H-NMR, mass and ESR spectra, magnetic susceptibility and molar conductivity measurements. The spectral data and magnetic measurements of the complexes indicate that, the ligand behaves either as neutral bidentate, monobasic bidentate, neutral tetradentate or bibasic tetradentate ligand. The geometries of the metal complexes are either square planar or octahedral. The antibacterial and antifungal activities of the compounds showed that, some of metal complexes exhibited a greater inhibitory effect than standard drugs (Tetracycline) for bacteria, (Amphotericin B) for fungi.

Keywords: Schiff base, metal complexes, synthesis, spectroscopic studies, ESR, antimicrobial

* Corresponding Author E-mail: asaeltabl@yahoo.com.

INTRODUCTION

There has been considerable interest in the synthesis of transition metal complexes of macrocyclic ligand systems because they play vital roles in biological systems [1]. Also, interest in these species stems largely from the enhanced kinetic and thermodynamic stability of their complexes relative to those of related open chain ligands. Macrocyclic complexes are also of interest because of the synthetic flexibility involved in their preparation which allows for systematic variation in parameters such as ring size, the nature of the donor atoms, and the steric and electronic effects associated with the groups located on the periphery of the macrocyclic ring [2]. There has been a spectacular growth in the interest in metal complexes with tetraazamacrocyclic ligands followed by extensive work on the metal controlled template synthesis of macrocyclic species [3]. Macrocyclic metal complexes using acetylacetone and 2,6 diacetyl pyridine have been reported [4]. Based upon the above consideration and in continuation to our earlier studies on the metal(II)/(III) macrocyclic complexes [5], This article aimed to synthesis, spectroscopic investigation and antimicrobial studies on metal complexes of Cu(II), Ni(II), Co(II), Cd(II), Mn(II), Zn(II), Fe(III) and Cr(III) of 7,12-dioxo-3,4,9,10-tetraphenyl-1,2,5,6-tetraazacyclododeca-2,4,8,10-tetraene-8,11-dicarbonitrile.

EXPERIMENTAL SECTION

Material

All the reagents employed for the preparation of the ligand and its complexes were of the best grade available and used without further purification.

Synthesis of the Schiff base Ligand [H_2L](1)

A hot ethanolic solution (50 mL) of acetocyanohydrazide (12.1 mmole, 1.2g) was added to a hot ethanol solutionic (50 mL) of benzil (12.1 mmole, 2.55 g). The mixture was refluxed for 3h after cooling, the yellow precipitate was filtered off, washed with ethanol and dried under vacuum over anhydrous $CaCl_2$, Scheme 1.^{1}H NMR (300MHz, $CHCl_3$): δ =10.94 [S, 1H, OH], 10.79 [S, 1H, NH], 7.9-7.6 [m, 20H, aromatic].From this data the ligand present in Keto-enol form in liquid state (DMSO) which was supported by the presence of NH and OH groups.

Synthesis of the Metal Complexes

Metal complexes were prepared by mixing a hot methanolic solution of the metal salts with the required amount of a hot ethanolic solution of the ligand to form 1:1 or 1:2 L/M (ligand /metal). The reaction mixture was then refluxed for 2-4 hr depending on the metal salt used. The precipitates formed were filtered off, washed with ethanol, and dried under vacuum over anhydrous $CaCl_2$.

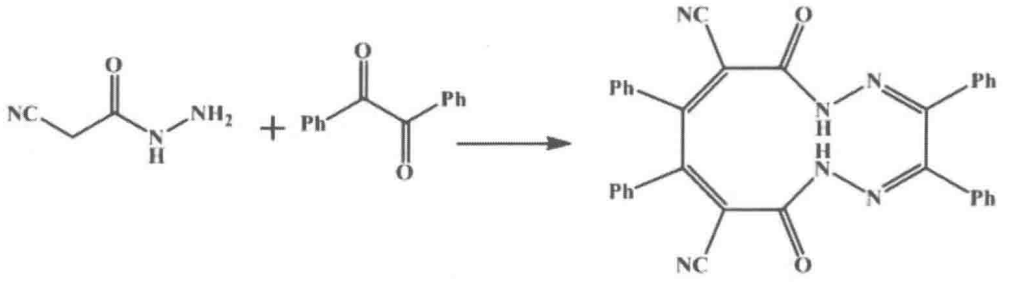

Scheme 1.Schematic representation for the formation of the ligand H_2L.

In-Vitro Antibacterial and Antifungal Activities

The investigation of the biological activities of the newly synthesized se ligand and its metal complexes and also their corresponding metal salts were carried out in the Botany Department Lab. of microbiology, Faculty of Science, El-Menoufia University, Egypt. The antibacterial and antifungal activities were investigated by disc diffusion method [6,7]. The antibacterial activities were done using gram positive bacteria (*Staphylococcus aurous*) and gram negative bacteria (*Escherichia coli*) and fungus (*Aspergillusflavus)* and yeast (*Candida albicans*) at 2000 ppm concentrations in DMSO. DMSO poured disc was used as negative control. The bacteria were subcultured in nutrient agar medium which was prepared using (g/L^{-1} distilled water) NaCl (5 g), peptone (5 g), beef extract (3 g), agar (20 g). The fungus was subcultured in Dox´s medium which was prepared using ($g.L^{-1}$ distilled water) yeast extract (1g), sucrose (30 g), $NaNO_3$, agar (20 g), KCl (0.5 g), KH_2PO_4 (1 g), $MgSO_4.7H_2O$ (0.5 g) and trace of $FeCl_3$ $.6H_2O$.The yeast was subcultured in MYGP medium which prepared using ($g.L^{-1}$ distilled water) yeast extract (3g), Malt extract (3 g), glucose (10 g), agar (20 g), peptone (5 g). These mediums were then sterilized by autoclaving at 120 ^{0}C for 15 min. After cooling to 45 ^{0}C the medium was poured into 90 mm diameter Petri dishes and incubated at 37 ^{0}C or 28 ^{0}C, respectively. After few hours, Petri dishes were stored at 4 ^{0}C. Microorganisms were spread over each dish by using sterile bent Loop rod. The test is carried out by placing filter paper disks with a known concentration of the compounds on the surface of agar plates inoculated with a test organism. Standard antibacterial drug (Tetracycline), antifungal drug (Amphotericin B) and solution of metal salts were also screened under similar conditions for comparison. The Petri dishes were incubated for 48-72 h. at 37 or 30 °C, respectively. The zone of inhibition was measured in millimeters carefully. All determinations were made in duplicated manner for all compounds. The average of the two independent readings was record.

Physical Measurements

The ligand and its metal complexes were analyzed for C, H, N, and Cl contents at the Micro-analytical Laboratory, Faculty of Science, Cairo University, Egypt. Analytical and physical data of the ligand and its metal complexes are reported in Table 1.

Table 1. Analytical and physical data of the ligand H_2L and its metal complexes

No.	Ligand/ Complexes	FW	Yield (%)	Analysis (%) / Found (calcd)					Λ^a_M
				C	H	N	M	Cl	
1	H_2L ($C_{34}H_{22}N_6O_2$)	546.6	72	74.5(74.7)	4.2(4.1)	15.5(15.4)	-	-	-
2	$[H_2LCu_2(OC(O)CH_3)_4].3H_2O$($C_{42}H_{40}Cu_2N_6O_{13}$)	963.9	87	52.2(52.3)	4.5(4.2)	8.9(8.7)	12.9(13.2)	-	11
3	$[H_2LCu(OC(O)CH_3)_2].H_2O$ ($C_{38}H_{30}CuN_6O_7$)	746.2	89	61.0(61.2)	4.2(4.1)	11.6(11.3)	8.3(8.5)	-	9
4	$[LCu_2Cl_2(H_2O)_2].H_2O$ ($C_{34}H_{26}Cl_2Cu_2N_6O_5$)	796.6	79	51.0(51.3)	3.4(3.3)	10.7(10.6)	15.9(16.0)	8.7(8.9)	15
5	$[H_2LCuCl_2].2H_2O$ ($C_{34}H_{26}Cl_2CuN_6O_4$)	717.1	77	56.9(57.0)	4.0(3.7)	11.8(11.7)	8.7(8.9)	9.8(9.9)	17
6	$[LCu_2(NO_3)_2(H_2O)_2].H_2O$ ($C_{34}H_{26}Cu_2N_8O_{11}$)	849.7	81	48.0(48.1)	3.3(3.1)	13.4(13.2)	14.7(15.0)	-	22
7	$H_2LCu_2(SO_4)_2(H_2O)_4$ ($C_{34}H_{30}Cu_2N_6O_{14}S_2$)	937.9	84	43.3(43.5)	3.5(3.2)	9.1(9.0)	13.4(13.6)	-	20
8	$[H_2LCu(SO_4)(H_2O)_2].2H_2O$ ($C_{34}H_{30}CuN_6O_{10}S$)	778.3	83	52.7(52.5)	4.1(3.9)	10.9(10.8)	8.0(8.2)	-	18
9	$H_2LNi_2(OC(O)CH_3)_4(H_2O)_4$ ($C_{42}H_{42}N_6Ni_2O_{14}$)	972.2	89	51.7(51.9)	4.1(4.4)	8.4(8.6)	11.9(12.1)	-	10
10	$H_2LNi_2(NO_3)_4(H_2O)_4C_{34}H_{30}N_{10}Ni_2O_{18}$	984.0	76	41.3(41.5)	3.4(3.1)	14.3(14.2)	11.7(11.9)	-	12
11	$H_2LCo_2Cl_4(H_2O)_4$ ($C_{34}H_{30}Cl_4Co_2N_6O_6$)	878.3	74	46.5(46.5)	3.6(3.4)	9.8(9.6)	13.1(13.4)	16.1(16.2)	14
12	$H_2LCo_2(NO_3)_4(H_2O)_4$ ($C_{34}H_{30}Co_2N_{10}O_{18}$)	984.5	75	41.3(41.5)	3.3(3.1)	14.4(14.2)	11.8(12.0)	-	18
13	$H_2LMn_2Cl_4.(H_2O)_4$ ($C_{34}H_{30}Cl_4Mn_2N_6O_6$)	870.3	79	46.(46.9)	3.7(3.5)	10.0(9.7)	12.4(12.6)	16.2(16.3)	19
14	$H_2LCr_2Cl_4(H_2O)_4$ ($C_{34}H_{30}Cl_4Cr_2N_6O_6$)	864.4	73	47.0(47.2)	3.5(3.5)	10.0(9.7)	11.9(12.0)	16.3(16.4)	20
15	$LFe_2Cl_4(H_2O)_4$ ($C_{34}H_{28}Cl_4Fe_2N_6O_6$)	870.1	78	46.8(46.9)	3.5(3.2)	9.8(9.7)	12.6(12.8)	16.2(16.3)	17
16	$[H_2LZn_2(OC(O)CH_3)_4].2H_2O$($C_{42}H_{38}N_6O_{12}Zn_2$)	949.5	71	53.0(53.1)	4.1(4.0)	9.0(8.9)	14.0(13.8)	-	8
17	$[LZnCl_2(H_2O)_2].3H_2O$ ($C_{34}H_{30}Cl_2N_6O_7Zn_2$)	836.3	73	48.6(48.8)	3.6(3.6)	10.2(10.1)	15.7(15.6)	8.4(8.5)	9

No.	Ligand/ Complexes	FW	Yield (%)	Analysis (%) / Found (calcd)					Λ^{a}_{M}
				C	H	N	M	Cl	
18	[LCd2Cl2(H2O)2].4H2O (C34H32Cd2Cl2N6O8)	948.4	78	43.0(43.1)	3.5(3.4)	9.0(8.9)	23.7(23.7)	7.4(7.5)	18
19	$[H_2LCdCl_2].3H_2O$ ($C_{34}H_{28}CdCl_2N_6O_5$)	783.9	82	52.0(52.1)	3.7(3.6)	10.9(10.7)	14.1(14.3)	9.0(9.0)	14
20	$[H_2LCd_2(OC(O)CH_3)_4].2H_2O$($C_{42}H_{38}Cd_2N_6O_{12}$)	1043.6	83	48.3(48.3)	3.8(3.7)	8.2(8.1)	21.3(21.5)	-	10
21	$[H_2LCd(OC(O)CH_3)_2].3H_2O$ ($C_{38}H_{34}CdN_6O_9$)	831.1	80	54.7(54.9)	4.4(4.1)	10.2(10.1)	13.7(13.5)	-	11
22	$[H_2LCd_2(NO_3)_4].2H_2O$ ($C_{34}H_{24}Cd_2N_{10}O_{15}$)	1037.4	79	39.2(39.4)	2.5(2.3)	13.6(13.5)	21.6(21.7)	-	17
23	$[H_2LCd_2(SO_4)_2].3H_2O$ ($C_{34}H_{28}Cd_2N_6O_{13}S_2$)	1017.6	81	40.0(40.1)	2.9(2.8)	8.5(8.3)	22.0(22.1)	-	14

Molar Conductance $=\Lambda_m$ ($\Omega^{-1}cm^2mol^{-1}$).

The metal ion contents of the complexes were determined by the previously reported methods [8]. IR spectra of the ligand and its metal complexes were measured using KBr discs with a Jasco FT/IR 300E Fourier transform infrared spectrophotometer covering the range 400–4000 cm^{-1} and in the 500–100 cm^{-1} region using polyethylene-sandwiched Nujol mulls on a Perkin Elmer FT-IR 1650 spectrophotometer. ^1H NMR spectrum was obtained on 300 MHz VARIAN NMR spectrometers. Chemical shifts (ppm) are reported relative to TMS. The mass spectrum was run at 70 eV with HP MODEL: MS. 5988A. The electronic spectra of the ligand and its complexes were obtained in Nujol mulls using a Shimadzu UV–240 UV–Vis recording spectrophotometer. Molar conductivities of the complexes in DMSO (10^{-3} M) were measured using a dip cell and a Bibby conductimeter MC1 at room temperature. Magnetic moments at 298 K were determined using the Gouy method by the following equation $\mu_{eff} = 2.84 \sqrt{\chi_m \times T}$ with $Hg[Co(SCN)_4]$ as calibrate. Diamagnetic corrections were estimated from Pascal's constant. [9] ESR measurements of solid complexes at room temperature were made using a Varian E-109 spectrophotometer, with DPPH as a standard material. TLC is used to confirm the purity of the compounds.

Results and Discussion

All metal complexes are stable in air and insoluble in common organic solvents but easily soluble in DMF and DMSO. The elemental and physical analyses (Table 1), spectral data (Table 2 ans 3), confirmed the suggested structures Figure 1.

Mass Spectra of the Ligand

The mass spectrum of the Schiff base ligand (1) revealed the molecular ion peak at m/e 547, which is coincident with the formula weight (546.6) for this ligand and supports the identity of the structure.

Infrared Spectra

The IR spectral data for the ligand (1) and its metal complexes are presented in Table 2. The IR spectrum of the ligand showed bands at3195, 1660 and 1600 cm^{-1} may be due to ν(NH), ν(C=O) and ν(C=N) groups, respectively [10]. The absence of any signals for hydroxy group indicates that the ligand is present in the keto-form in the solid state. The spectra of solid complexes are compared with those of the ligand in order to know the mode of bonding. The spectra showed that, the ligand behaved either as:

1. Neutral bidentate ligand, coordinating through C=O and C=N of one side of the ligand (complexes 3, 5,8, 17,19, 21), the mode of coordination was suggested by the following evidence: i) ν(C=O)and ν(C=N) of one side of the ligand were shifted to lower wave number with decreasing their intensities, while the other ones found almost at their original place, indicating that, only one of each pair were involved in the coordination, [11]. ii) ν(NH) of one side of the ligand was shifted to higher wave